Electronic Supplementary Information for:

Is the contribution of *cis* and *trans* protonated 5-methylcytosine-SO_3^- isomers equal to thymine-SO_3^- under bisulfite conditions? A theoretical perspective

Lingxia Jin[a,b] Lu Wang[a] Caiying Zhang[a] Wenliang Wang[a,*] Suotian Min[b] Daodao Hu[a]

[a]*Key Laboratory for Macromolecular Science of Shaanxi Province, School of Chemistry and Chemical Engineering, Shaanxi Normal University, Xi'an 710062*

[b]*School of Chemical and Environmental Sciences, Shaanxi University of Technology, Hanzhong 723001*

*Corresponding author: Wenliang Wang Tel: +86-29-81530815, Fax: +86-81530727

E-mail: wlwang@snnu.edu.cn.

Table S1 Relative Energies (in kJ·mol^{-1}) for the Two Water-mediated Hydrolytic Deamination of CytN3^{+}-SO_3^{-} with the HSO_3^{-} Group Both in the Gas and Aqueous Phases

Table S2 Relative Energies (in kJ·mol^{-1}) for One Water-mediated Path A (1w-path A) Both in the Gas and Aqueous Phases

Table S2 Relative Energies (in kJ·mol^{-1}) for One Water-mediated Path A' (1w-path A') Both in the Gas and Aqueous Phases

Fig. S1 Optimized structures of *cis and trans* 5-MeCytN3^{+}-SO_3^{-} isomers in the aqueous phase are at B3LYP/6-311++G(d,p) level.

Fig. S2 Optimized structures (bond distances in Å) in the aqueous phase for the hydrolytic deamination of *cis* 5-MeCytN3^{+}-SO_3^{-} isomer with the HSO_3^{-} group (path A-the HSO_3^{-} group toward the left side of *cis* 5-MeCytN3^{+}-SO_3^{-} isomer) at the B3LYP/6-311++G(d, p) level.

Fig. S3 Optimized structures (bond distances in Å) in the aqueous phase for the hydrolytic deamination of *cis* 5-MeCytN3^{+}-SO_3^{-} isomer with the HSO_3^{-} group (path B-the HSO_3^{-} group toward the above side of *cis* 5-MeCytN3^{+}-SO_3^{-} isomer) at the B3LYP/6-311++G(d, p) level.

Fig. S4 Optimized structures (bond distances in Å) in the aqueous phase for the hydrolytic deamination of *cis* 5-MeCytN3^{+}-SO_3^{-} isomer with the HSO_3^{-} group (path C-the HSO_3^{-} group toward the right side of *cis* 5-MeCytN3^{+}-SO_3^{-} isomer) at the B3LYP/6-311++G(d, p) level.

Fig. S5 Optimized structures (bond distances in Å) in the aqueous phase for the hydrolytic deamination of *trans* 5-MeCytN3^{+}-SO_3^{-} isomer with the HSO_3^{-} group (path A'-the HSO_3^{-} group toward the left side of *trans* 5-MeCytN3^{+}-SO_3^{-} isomer) at the B3LYP/6-311++G(d, p) level.

Fig. S6 Optimized structures (bond distances in Å) in the aqueous phase for the hydrolytic deamination of *trans* 5-MeCytN3^{+}-SO_3^{-} isomer with the HSO_3^{-} group (path B'-the HSO_3^{-} group toward the above side of *trans* 5-MeCytN3^{+}-SO_3^{-} isomer) at the B3LYP/6-311++G(d, p) level.

Fig. S7 Optimized structures (bond distances in Å) in the aqueous phase for the hydrolytic deamination of *trans* 5-MeCytN3^{+}-SO_3^{-} isomer with the HSO_3^{-} group (path C'-the HSO_3^{-} group toward the right side of *trans* 5-MeCytN3^{+}-SO_3^{-} isomer) at the B3LYP/6-311++G(d, p) level.

Fig. S8 Optimized stationary structures (bond distances in Å) in the aqueous phase for two water-

mediated path A (2w-path A) are at B3LYP/6-311++G(d,p) level.

Fig. S9 Optimized stationary structures (bond distances in Å) in the aqueous phase for two water-mediated path A' (2w-path A') are at B3LYP/6-311++G(d,p) level.

Table S1 Relative Energies [a] (in kJ·mol^{-1}) for the Two Water-mediated Hydrolytic Deamination of CytN3^{+}-SO_3^{-} with the HSO_3^{-} Group Both in the Gas and Aqueous Phases

System	MP2//B3LYP[b]			PCM[c]	
	ΔE^{g}	ΔG^{g}	$\Delta G^{g\neq}$	$\Delta G^{s\text{-}a}$	$\Delta G^{s\text{-}a\neq}$
2w-path A					
R[d]+2H_2O	0.00	0.00		0.00	
2w-A-RC	-354.24	-192.44		35.03	
2w-A-TS1	-263.53	-94.08		120.30	
2w-A-IM1	-265.49	-101.21		102.75	
2w-A-TS2	-193.38	-25.03		190.93	
2w-A-IM2	-322.09	-155.50		60.41	
2w-A-TS3	-334.34	-163.09		106.18	
2w-A-P	-376.69	-218.57		59.82	
2w-A-RC→2w-A-IM1			98.36		85.27
2w-A-IM1→2w-A-IM2			76.18		88.18
2w-A-IM1→2w-A-P			-7.59		45.77

[a] ΔG^{g}, ΔE^{g}, and $\Delta G^{g\neq}$ are relative free energy, relative energy, and activation free energy in the gas phase, respectively. $\Delta G^{s\text{-}a}$ and $\Delta G^{s\text{-}a\neq}$ are relative free energy and activation free energy with PCM model based on the optimized geometries in the aqueous phase, respectively. [b] MP2/6-311++G(3df,3pd)//B3LYP/ 6-311++G(d,p) level. [c] MP2/6-311++G(3df,3pd)//B3LYP/6-311++G(d,p) with PCM model. [d] denotes CytN3^{+}-SO_3^{-} +H_2O+HSO_3^{-}.

Table S2 Relative Energies [a] (in kJ·mol^{-1}) for One Water-mediated Path A (1w-path A) Both in the Gas and Aqueous Phases

System	MP2//B3LYP [b]			PCM[c]	
	ΔE^{g}	ΔG^{g}	$\Delta G^{g\neq}$	$\Delta G^{s\text{-}a}$	$\Delta G^{s\text{-}a\neq}$
1w-path A					
R[d]+H_2O	0.00	0.00		0.00	0.00
1w-A-RC	-219.84	-203.55		-112.38	6.35
1w-A-TS1	-273.20	-86.97		-33.94	98.02
1w-A-IM1	-252.75	-144.06		-67.80	61.65
1w-A-TS2	-273.34	-120.17		-60.44	73.26
1w-A-IM2	-280.36	-145.28		-83.52	45.82
1w-A-TS3	-275.23	-150.61		-81.73	48.65
1w-A-IM3	-274.50	-147.54		-74.19	54.25
1w-A-TS4	-286.76	-145.54		-72.23	58.34
1w-A-IM4	-255.98	-154.06		-116.18	16.71
1w-A-TS5	-284.74	-119.72		-64.07	74.62
1w-A-IM5	-289.85	-153.08		-92.06	41.02
1w-A-TS6	-283.89	-155.69		-101.78	31.37
1w-A-IM6	-256.16	-151.06		-101.87	30.36
1w-A-TS7	-348.36	-123.07		-72.65	59.57
1w-A-P	-322.97	-224.89			
1w-A-RC→1w-A-IM1			116.58		91.67
1w-A-IM1→1w-A-IM2			23.89		11.61
1w-A-IM2→1w-A-IM3			-5.33		2.83
1w-A-IM3→1w-A-IM4			2.00		4.09
1w-A-IM4→1w-A-IM5			34.34		57.91
1w-A-IM5→1w-A-IM6			-2.61		-9.65
1w-A-IM6→1w-A-P			27.99		29.21

[a] ΔG^{g}, ΔE^{g}, and $\Delta G^{g\neq}$ are relative free energy, relative energy, and activation free energy in the gas phase, respectively. $\Delta G^{s\text{-}a}$ and $\Delta G^{s\text{-}a\neq}$ are relative free energy and activation free energy with PCM model based on the optimized geometries in the aqueous phase, respectively. [b] MP2/6-311++G(3df,3pd)//B3LYP/ 6-311++G(d,p) level. [c] MP2/6-311++G(3df,3pd)//B3LYP/6-311++G(d,p) with PCM model. [d] denotes *cis* 5-MeCytN3^{+}-SO_3^{-} isomer +H_2O+HSO_3^{-}.

Table S3 Relative Energies [a] (in kJ·mol^{-1}) for One Water-mediated Path A' (1w-path A') Both in the Gas and Aqueous Phases

System	MP2//B3LYP [b]			PCM[c]	
	ΔE^{g}	ΔG^{g}	$\Delta G^{g\neq}$	$\Delta G^{s\text{-}a}$	$\Delta G^{s\text{-}a\neq}$
1w-path A'					
R [d] +H_2O	0.00	0.00		0.00	
1w-A'-RC	-312.25	-195.26		-1.40	
1w-A'-TS1	-218.69	-84.70		107.56	
1w-A'-IM1	-276.65	-145.48		66.70	
1w-A'-TS2	-256.93	-122.31		75.31	
1w-A'-IM2	-277.22	-146.37		54.26	
1w-A'-TS3	-284.23	-151.97		56.75	
1w-A'-IM3	-279.04	-149.14		59.95	
1w-A'-TS4	-280.65	-149.00		34.35	
1w-A'-IM4	-290.38	-155.58		47.57	
1w-A'-TS5	-260.05	-122.42		77.10	
1w-A'-IM5	-287.49	-153.27		47.02	
1w-A'-TS6	-292.48	-156.21		11.61	
1w-A'-IM6	-286.22	-151.22		35.43	
1w-A'-TS7	-244.57	-110.52		100.24	
1w-A'-P	-352.41	-227.43		-25.25	
1w-A'-RC→1w-A'-IM1			110.56		108.96
1w-A'-IM1→1w-A'-IM2			23.17		8.61
1w-A'-IM2→1w-A'-IM3			-5.60		2.49
1w-A'-IM3→1w-A'-IM4			0.14		-25.60
1w-A'-IM4→1w-A'-IM5			33.16		29.53
1w-A'-IM5→1w-A'-IM6			-2.94		-35.41
1w-A'-IM6→1w-A'-P			40.70		64.81

[a] ΔG^{g}, ΔE^{g}, and $\Delta G^{g\neq}$ are relative free energy, relative energy, and activation free energy in the gas phase, respectively. $\Delta G^{s\text{-}a}$ and $\Delta G^{s\text{-}a\neq}$ are relative free energy and activation free energy with PCM model based on the optimized geometries in the aqueous phase, respectively. [b] MP2/6-311++G(3df,3pd)//B3LYP/ 6-311++G(d,p) level. [c] MP2/6-311++G(3df,3pd)//B3LYP/6-311++G(d,p) with PCM model. [d] denotes *trans* 5-MeCytN3^{+}-SO_3^{-} isomer +H_2O+HSO_3^{-}.

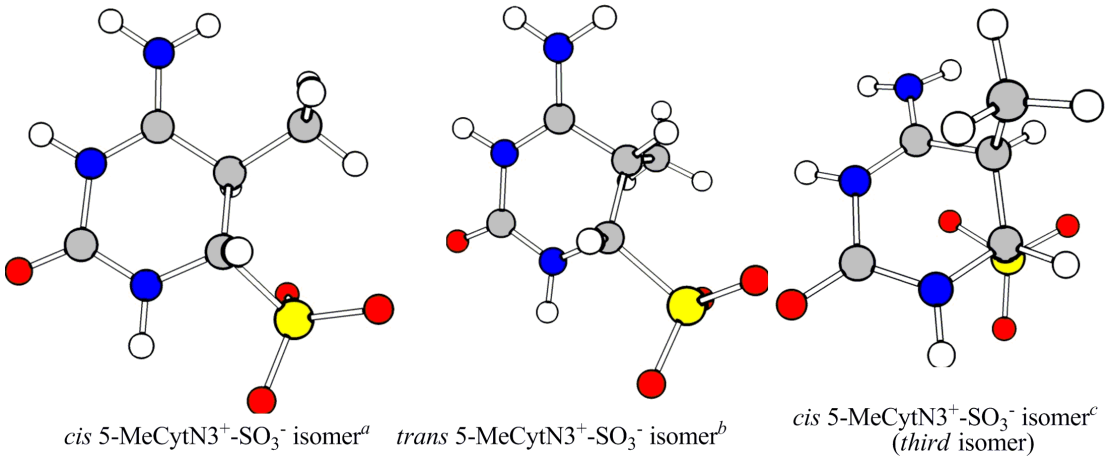

Fig. S1

[a] 5-H *cis* to 6-SO_3^-(both the CH_3 and SO_3 occupy equatorial positions); [b] 5-H *trans* to 6-SO_3^- (the CH_3 occupies axial position and the SO_3 occupies equatorial position);[c] 5-H *cis* to 6-SO_3^- (both the CH_3 and SO_3 occupy axial positions).

We have designed various initial deamination routes of *third* 5-MeCytN3$^+$-SO_3^- isomer for optimization, but the hydrolytic product of each step is always similar to that of *cis* 5-MeCytN3$^+$-SO_3^- isomer, which may result from the low free energy barrier of the conversion between *third* and *cis* 5-MeCytN3$^+$-SO_3^- isomers.[1] Thus, our interest has been focused on the hydrolytic deamination routes of *cis* and *trans* 5-MeCytN3$^+$-SO_3^- isomers in the this study.

(1) L. X. Jin, W. L. Wang, D. D Hu and S. T. Min, *J. Phys. Chem. B.*, 2013, **117**, 3.

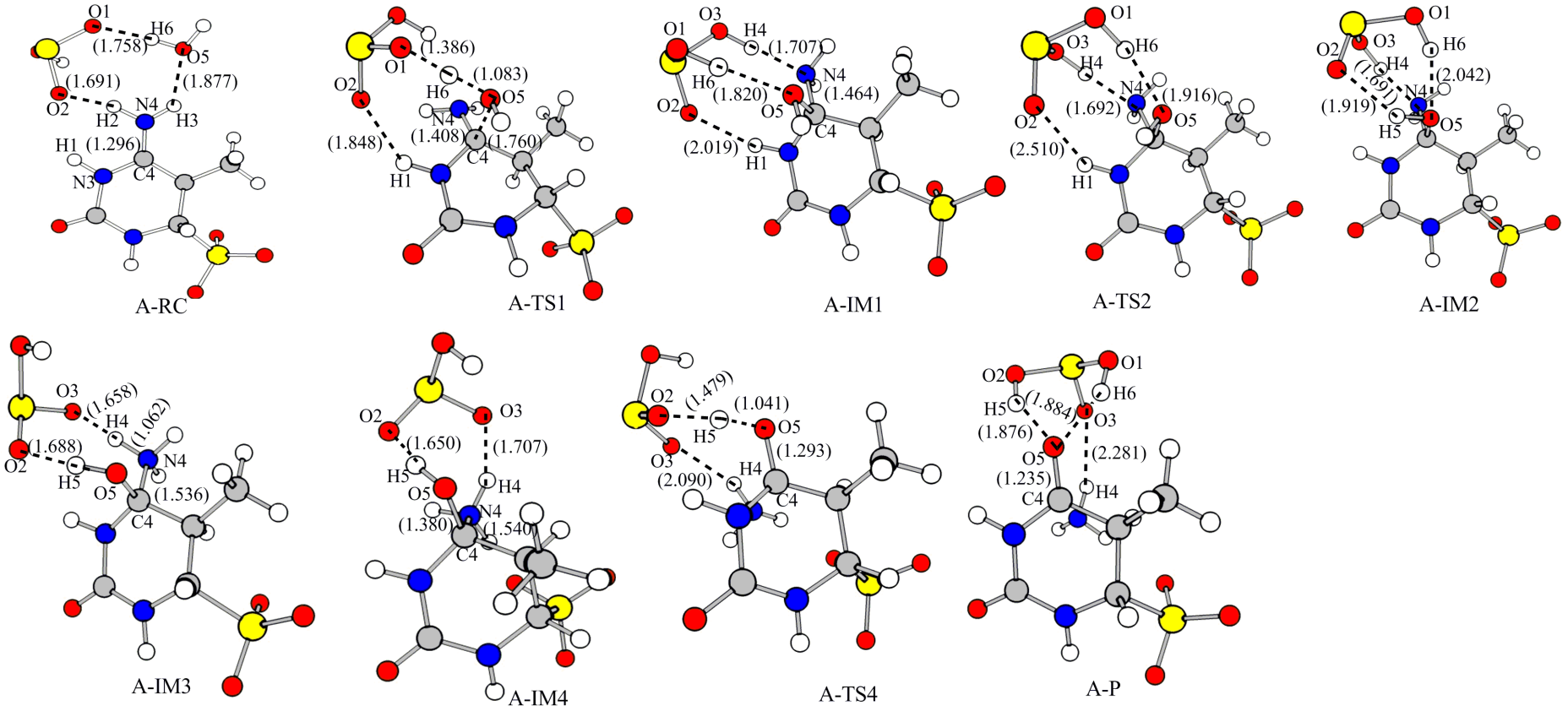

Fig. S2

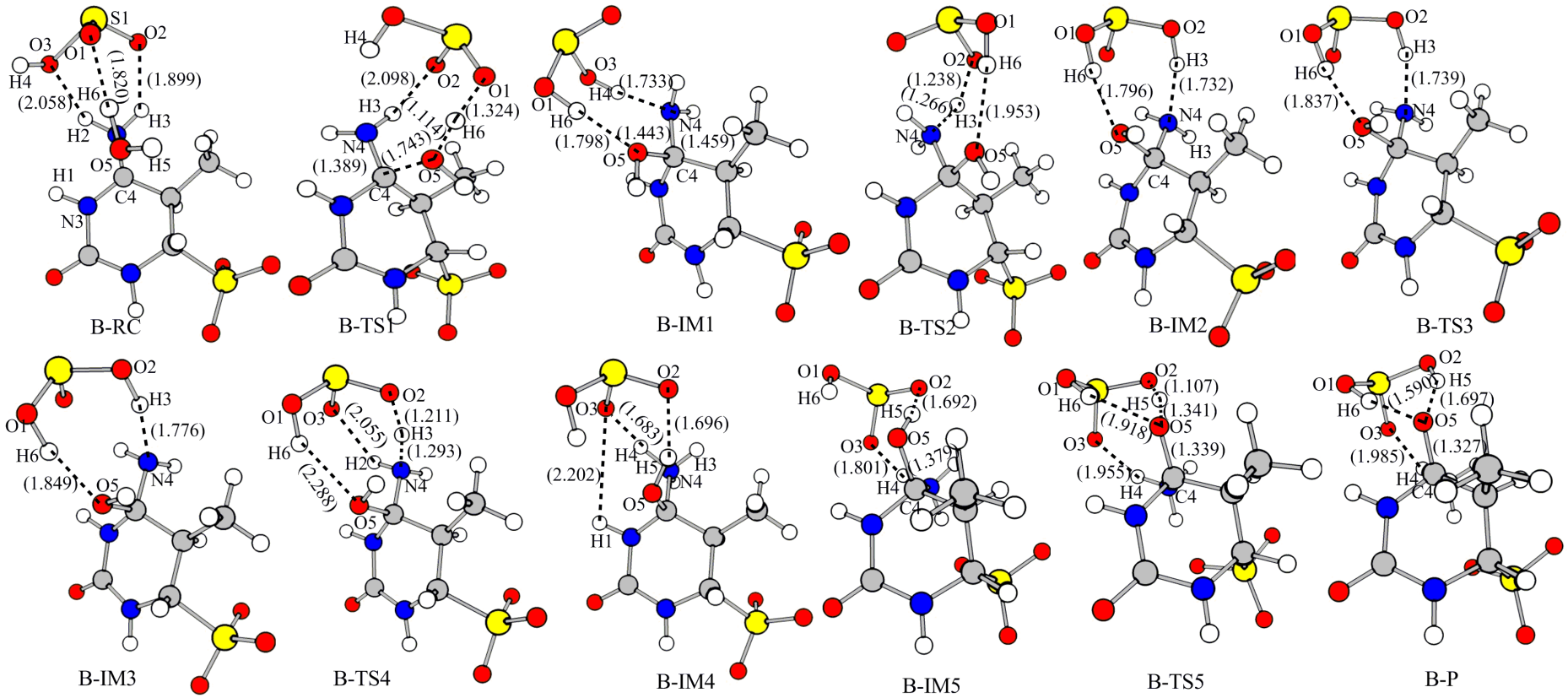

Fig. S3

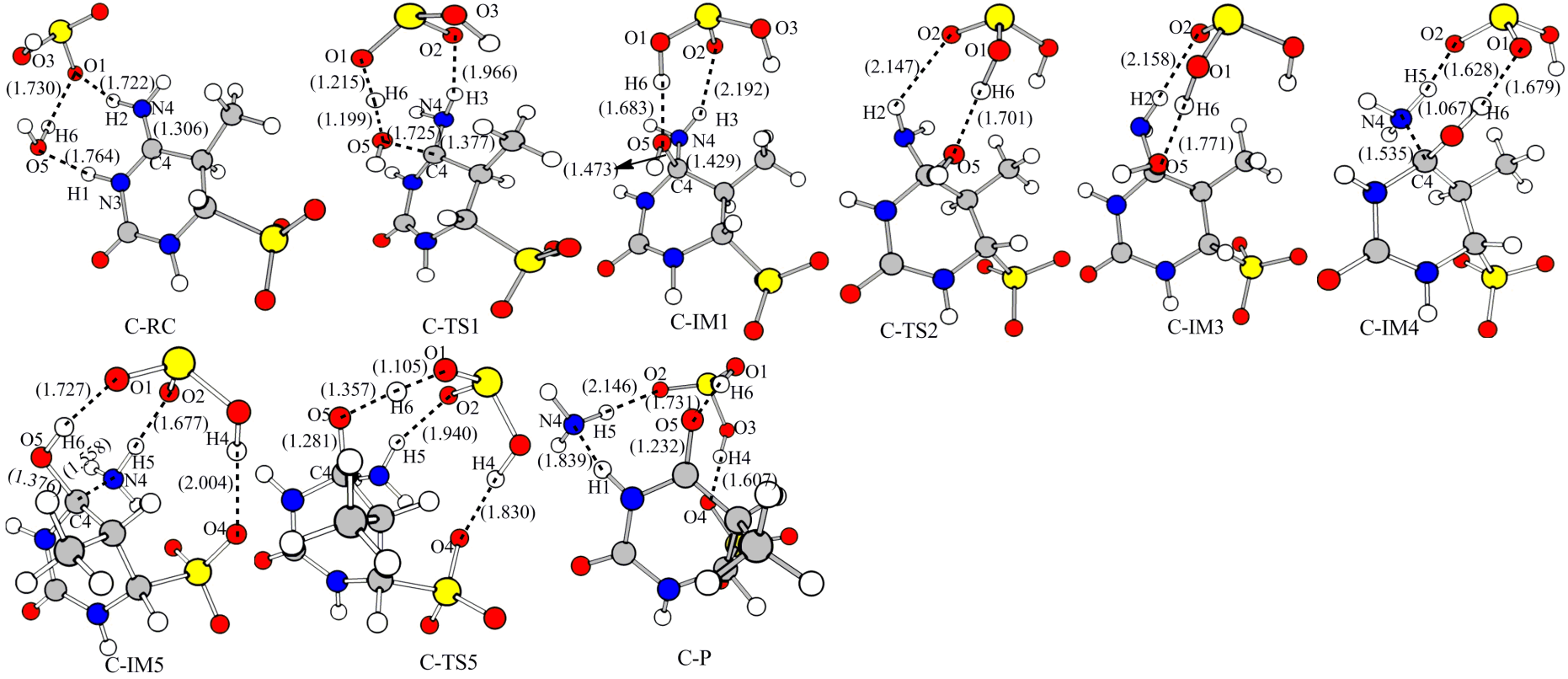

Fig. S4

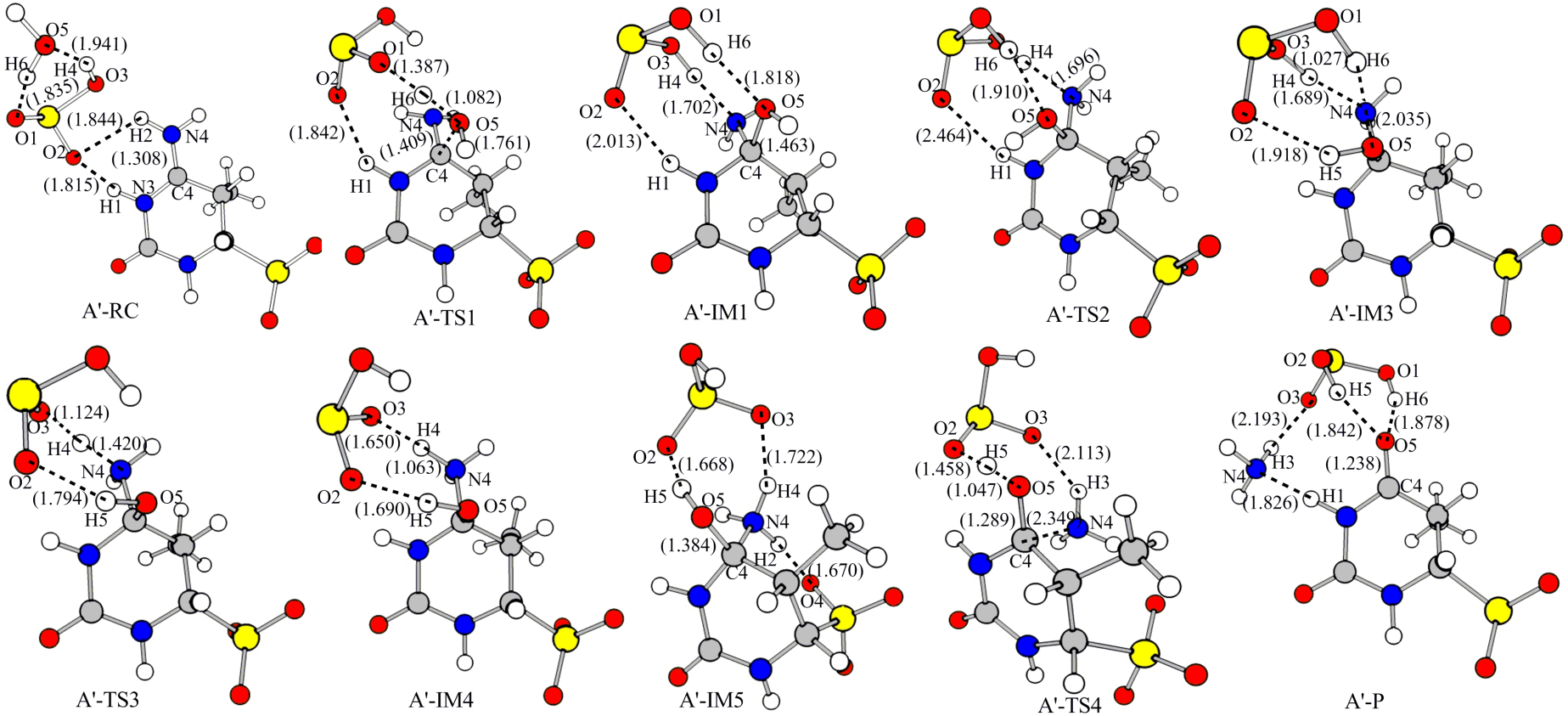

Fig. S5

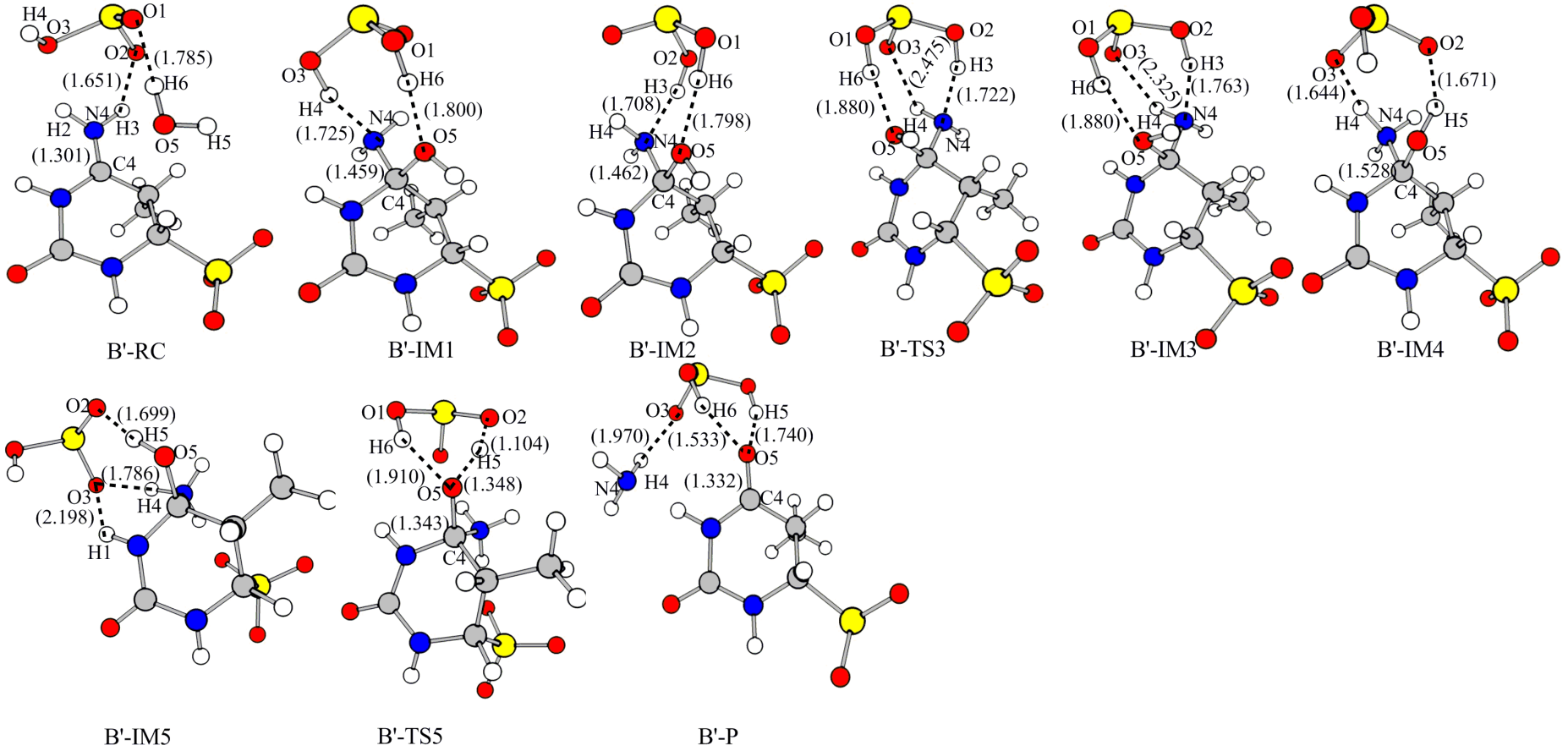
H4
O3
O1
O2
(1.785)
(1.651)
H6
N4
H2
H3
O5
H5
(1.301)
C4
B'-RC
O3
O1
H6
H4
N4
(1.800)
(1.725)
O5
(1.459)
C4
B'-IM1
O1
O2
H3
H6
(1.708)
(1.798)
H4
N4
O5
(1.462)
C4
B'-IM2
O1
O3
O2
(2.475)
H3
H6
(1.880)
(1.722)
H4
O5
N4
B'-TS3
O1
O2
O3
(2.325)
H3
(1.763)
H6
(1.880)
H4
N4
O5
B'-IM3
O3
O2
(1.644)
(1.671)
H4
N4
H5
O5
(1.528)
C4
B'-IM4
O2
(1.699)
H5
O5
(1.786)
O3
H4
(2.198)
H1
B'-IM5
O1
O2
H6
(1.104)
H5
(1.910)
O5
(1.348)
(1.343)
C4
B'-TS5
O3
H6
H5
(1.970)
(1.533)
(1.740)
O5
N4
H4
(1.332)
C4
B'-P

Fig. S6

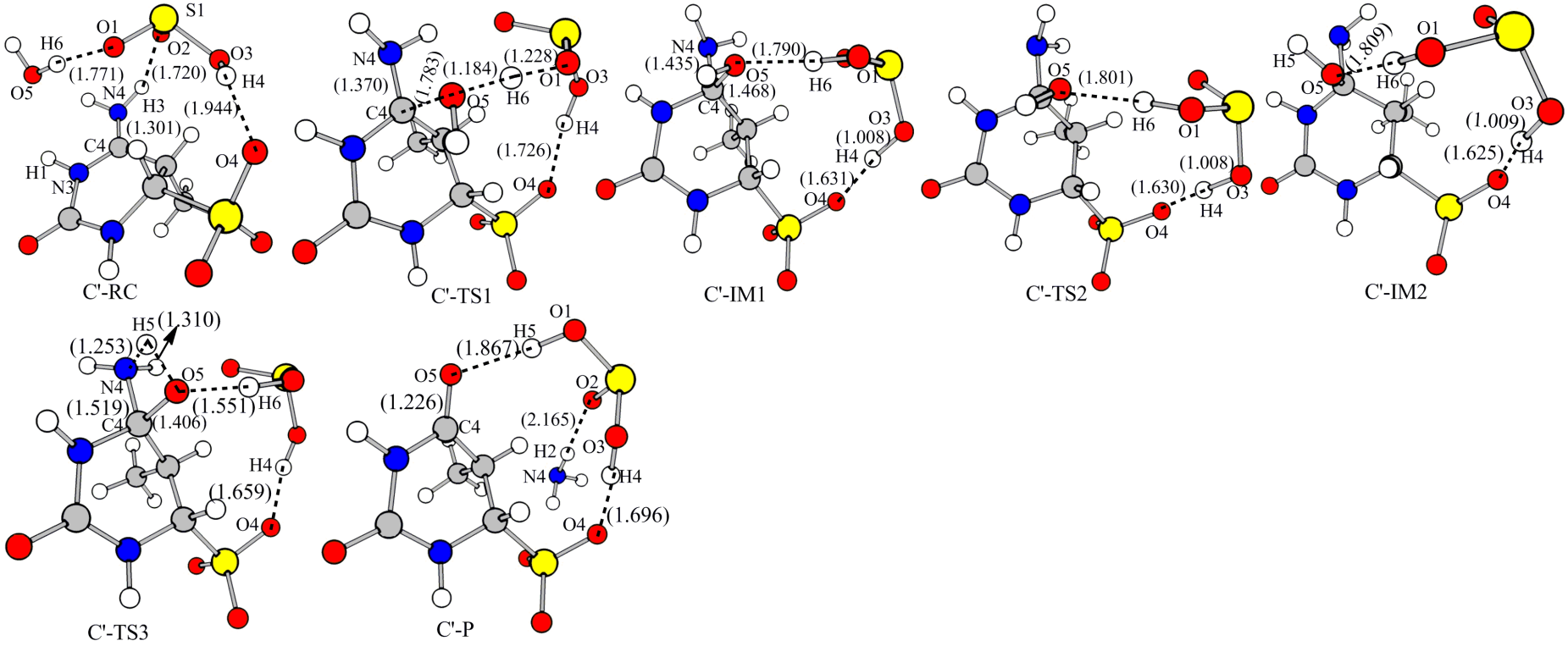

Fig. S7

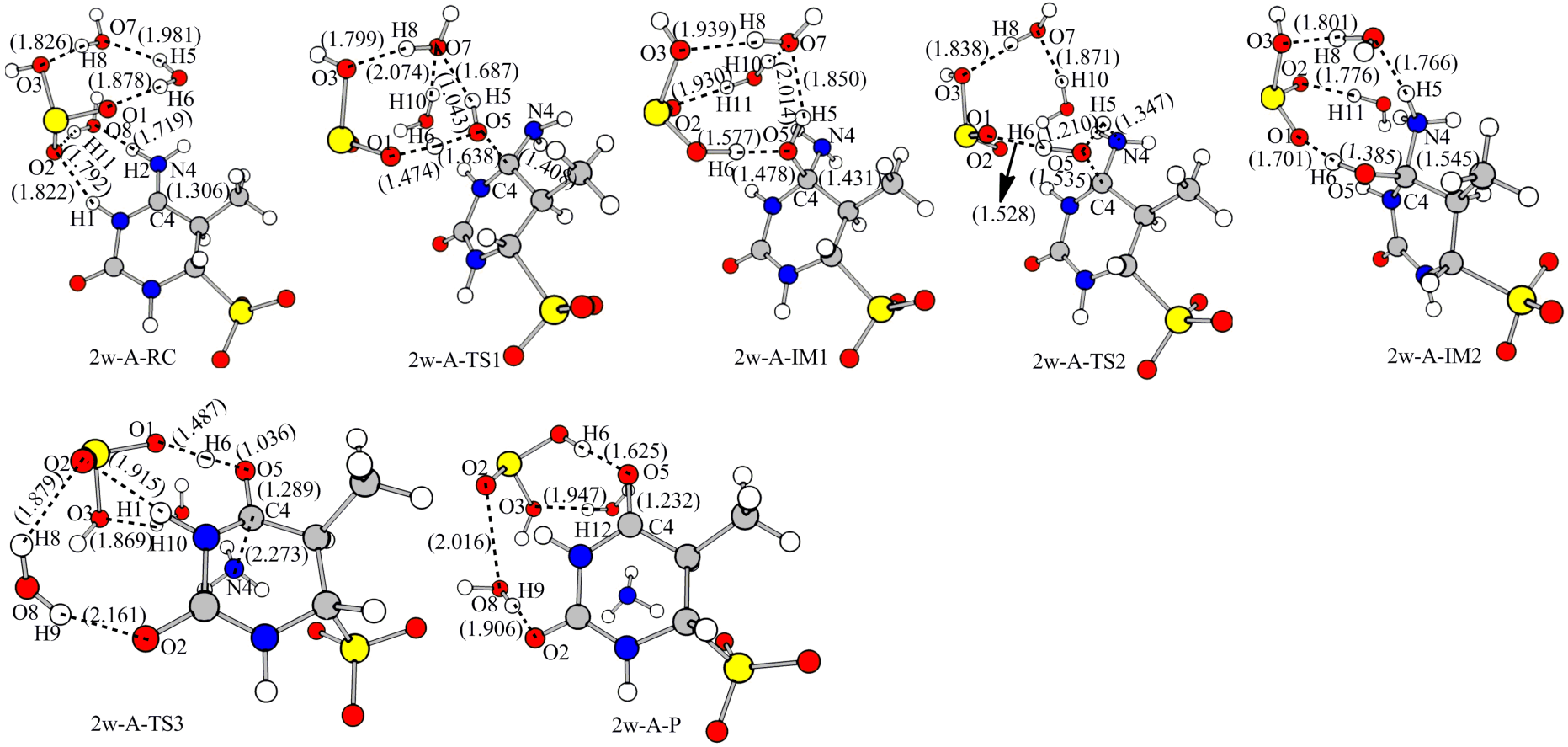

Fig. S8

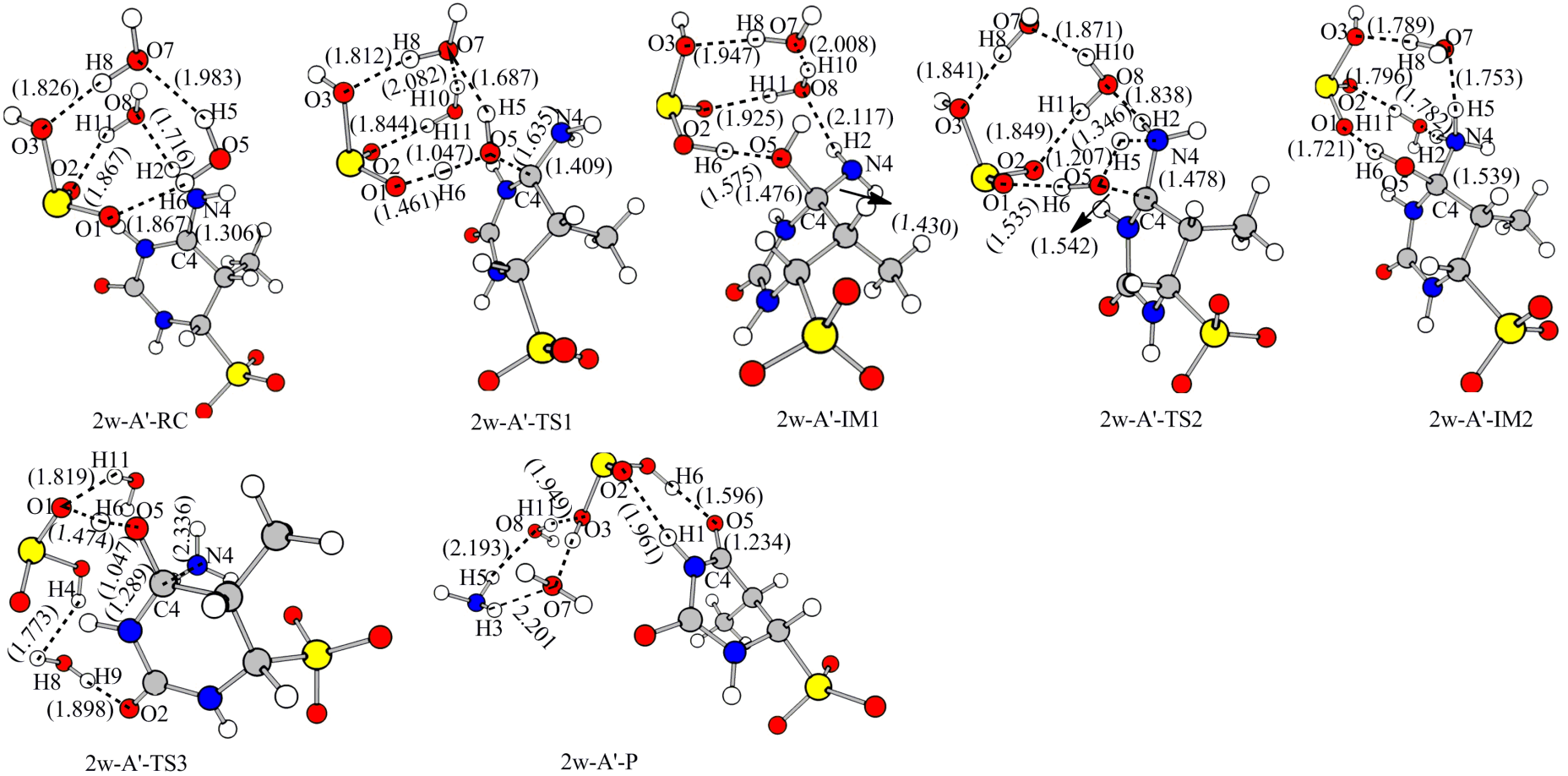

Fig. S9